

THE REGIME OF THE WESTERN PART OF THE ROSS ICE SHELF DRAINAGE SYSTEM*

By M. GIOVINETTO,

(Geophysical and Polar Research Center, Department of Geology and Department of Geography, University of Wisconsin, Madison, Wisconsin, U.S.A.)

EDWIN S. ROBINSON

(Geophysical and Polar Research Center, University of Wisconsin, Madison, Wisconsin, U.S.A.)†

and C. W. M. SWITHINBANK

(Scott Polar Research Institute, Cambridge, England)

ABSTRACT. The net mass budget is estimated for the western part of the Ross Ice Shelf drainage system. The area of the system is $(1.75 \pm 0.26) \times 10^6$ km², and the drainage periphery extends along the eastern flank of the Trans-Antarctic Mountains between lat. $77^\circ 58' \text{ S}$, long. $164^\circ 37' \text{ E}$. and lat. $85^\circ 27' \text{ S}$, long. $147^\circ 50' \text{ W}$. Ice discharge is estimated from vertical cross-sections and corresponding ice-movement data for eight outlet glaciers. Free-air gravity anomalies, corrected for the effect of terrain above the glacier surface, are used to determine cross-sections of valleys by comparison with theoretical gravity profiles for several two-dimensional valley models. These data provide a basis for estimating the rate of ice discharge from the plateau, which is compared with the estimated rate of net accumulation at the surface, to determine the net budget of the ice sheet in the region. Representative mean rates of ice discharge measured in different types of glaciers are approximately 0.25×10^{15} g. km⁻¹ yr.⁻¹ in outlet glaciers with large basins, and 0.05×10^{15} g. km⁻¹ yr.⁻¹ in outlet glaciers with small basins. Taking into account the snowshed area and the rate of accumulation, the rate of ice discharge in cirque and piedmont glaciers is estimated at about 0.02×10^{15} g. km⁻¹ yr.⁻¹. The difference $((48 \pm 29) \times 10^{15}$ g. yr.⁻¹) between mass input $((96 \pm 25) \times 10^{15}$ g. yr.⁻¹) and mass output $((48 \pm 15) \times 10^{15}$ g. yr.⁻¹) is large enough relative to the estimated standard error to indicate a probable positive net budget.

RÉSUMÉ. Le régime du système de drainage de la partie ouest du Ross Ice Shelf. Le bilan de masse net est estimé pour le système de drainage de la partie ouest du Ross Ice Shelf. La surface de ce système est de $1,75 \pm 0,26 \times 10^6$ km², et sa périphérie s'étend le long des flancs est des Trans-Antarctic Mountains entre $77^\circ 58' \text{ S}$, $164^\circ 37' \text{ E}$ et $85^\circ 27' \text{ S}$, $147^\circ 50' \text{ W}$. Le débit de glace est estimé à partir de sections droites verticales et les données correspondantes du mouvement pour huit glaciers effluents. Les anomalies gravimétriques à l'air libre, corrigées de l'effet topographique du terrain situé au-dessus de la surface des glaciers, ont été utilisées pour déterminer les sections droites des vallées par comparaison avec des profils gravimétriques théoriques pour plusieurs modèles bidimensionnels de vallée. Ces données forment une base pour l'estimation de la valeur du débit de la glace du plateau, débit comparé à la valeur estimée de l'accumulation nette à la surface, pour déterminer le bilan net de la couverture de glace de cette région. Les valeurs moyennes représentatives de débit de glace mesurées pour différents types de glaciers sont environ de $0,25 \times 10^{15}$ g km⁻¹ an⁻¹ pour des glaciers effluents avec de grands bassins de drainage, et de $0,05 \times 10^{15}$ g km⁻¹ an⁻¹ pour des glaciers effluents avec de petits bassins de drainage. Tenant compte de la surface enneigée et de la valeur de l'accumulation, la valeur du débit de glace des glaciers de cirque et de piedmont est estimée à environ $0,02 \times 10^{15}$ g km⁻¹ an⁻¹. La différence $48 \pm 29 \times 10^{15}$ g an⁻¹ entre l'apport de masse $96 \pm 25 \times 10^{15}$ g an⁻¹ et la sortie de masse $48 \pm 15 \times 10^{15}$ g an⁻¹, est assez large relativement à l'erreur standard estimée pour indiquer un bilan net positif probable.

ZUSAMMENFASSUNG. Der Massenhaushalt im Westteil des Einzugsgebietes des Ross Ice Shelf. Für den Westteil des Einzugsgebietes des Ross Ice Shelf wird der Netto-Massenhaushalt abgeschätzt. Die Fläche des Gebietes beträgt $(1,75 \pm 0,26) \times 10^6$ km²; seine Grenze erstreckt sich längs der Ostflanke der Trans-Antarctic Mountains zwischen $77^\circ 58'$ südl. Br., $164^\circ 37'$ östl. L. und $85^\circ 27'$ südl. Br., $147^\circ 50'$ westl. L. Der Eisausstoss wird aus vertikalen Querprofilen und zugehörigen Fließgeschwindigkeitswerten für acht Auslass-Gletscher abgeschätzt. Zur Bestimmung der Talquerschnitte werden Freiluftanomalien der Schwere, korrigiert um den Einfluss der Massen über der Gletscheroberfläche, benutzt; dabei werden theoretische Schwerkraftprofile für verschiedene zweidimensionale Talmodelle zum Vergleich herangezogen. Diese Daten ergeben eine Grundlage für die Abschätzung des Eisausstosses vom Polplateau, der mit der abgeschätzten Netto-Akkumulation auf der Oberfläche verglichen wird, um den Netto-Haushalt des Inlandeises in diesem Gebiet zu bestimmen. Repräsentative Mittelwerte des Eisausstosses, gemessen an Gletschern verschiedenen Typs, sind ungefähr $0,25 \times 10^{15}$ g km⁻¹ pro Jahr für Auslass-Gletscher mit grossem Becken und $0,05 \times 10^{15}$ g km⁻¹ pro Jahr für Auslass-Gletscher mit kleinem Becken. Unter Berücksichtigung der Akkumulationsfläche und

* Geophysical and Polar Research Center, University of Wisconsin, Contribution No. 144.

† Now at Department of Geophysics, College of Mines and Mineral Industries, University of Utah, Salt Lake City, Utah, U.S.A.

-menge lässt sich der Eisausstoss in Kar- und Fussflächengletschern auf ca. $0,02 \times 10^{15}$ g km^{-1} pro Jahr abschätzen. Der Unterschied von $(48 \pm 29) \times 10^{15}$ g pro Jahr zwischen dem Auftrag von $(96 \pm 25) \times 10^{15}$ g pro Jahr und dem Ausstoss von $(48 \pm 15) \times 10^{15}$ g pro Jahr ist im Verhältnis zu den abgeschätzten mittleren Fehlern gross genug um einen positiven Massenhaushalt als wahrscheinlich annehmen zu lassen.

INTRODUCTION

Between 1957 and 1963 various field parties have carried out glaciological studies in the western region of the Ross Ice Shelf drainage system (Fig. 1), an area drained by glaciers feeding into the Ross Ice Shelf. Measurements of ice movement were made on the eight

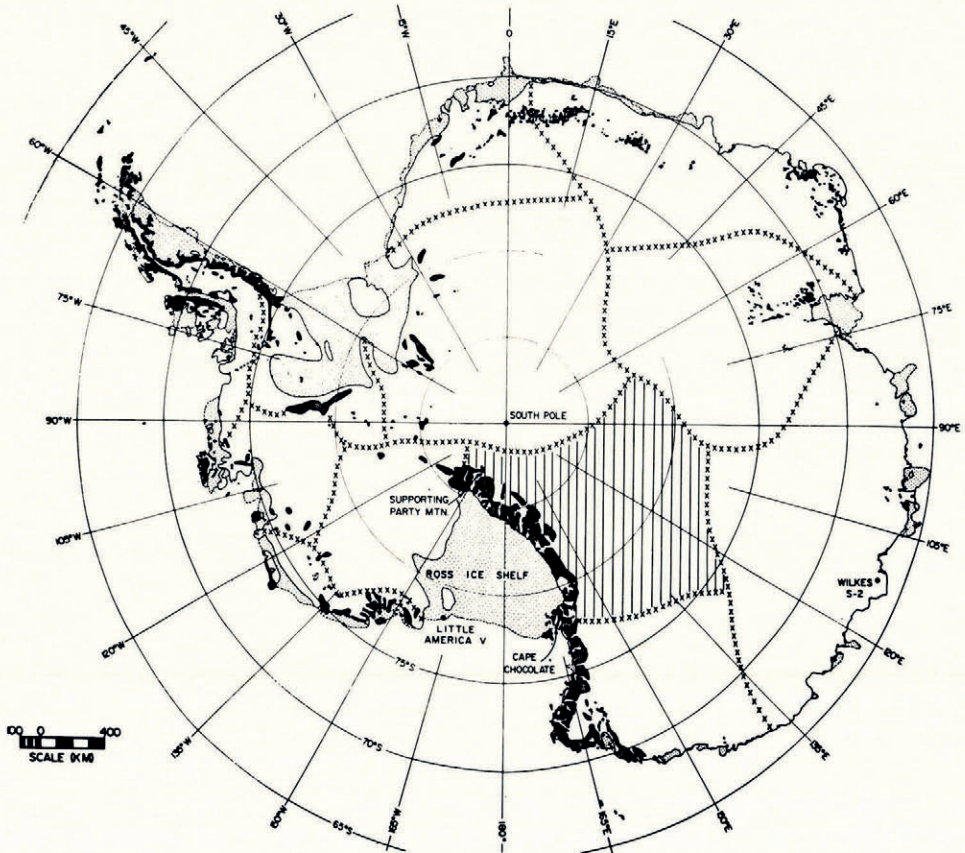


Fig. 1. The drainage divides in Antarctica (modified after Giovinetto (1964[b])) are shown with crosses. The area of the western part of the Ross Ice Shelf drainage system is vertically shaded. The drainage periphery extends from Cape Chocolate to Supporting Party Mountain

glaciers shown in Figure 2 in 1958 (Wilson and Crary, 1961) and in 1962–63 (Swithinbank, 1963), and gravity observations were made across the valleys to measure valley cross-sections. These data provide a basis for estimating the rate of ice discharge from the plateau, which is compared with the estimated rate of net accumulation at the surface to determine the net budget of the ice sheet in the region. The gravity analysis is treated in some detail, but accumulation values (Giovinetto, 1963) and ice-movement measurements (Swithinbank, 1963) have been described earlier and are only briefly reviewed.

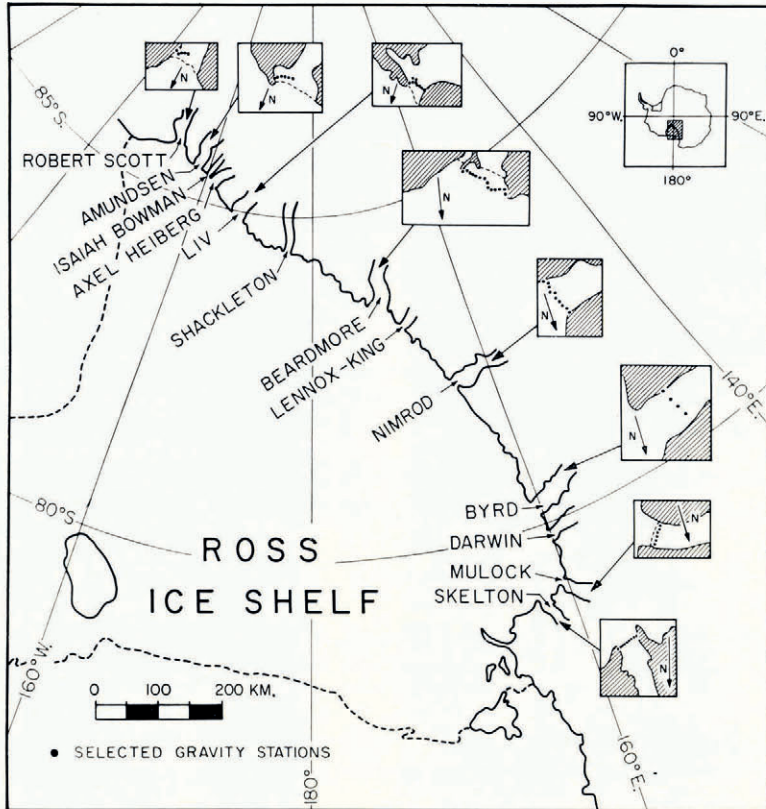


Fig. 2. Glaciers flowing into the Ross Ice Shelf upon which the gravity and ice-movement measurements were made

REDUCTION OF GRAVITY DATA

The data

Values of observed gravity accurate to ± 2 mgal were obtained at 144 stations (Appendix) from readings of the Worden gravimeter No. 291 adjusted to a base value of 982.992 gal at the McMurdo pendulum station (lat. $77^{\circ} 53' 1''$ S., long. $166^{\circ} 45' 3''$ E.; 11 m.; Fig. 1). The station positions were established by triangulation measurements adjusted to control points from sun shots. Absolute elevations of several stations on the ice shelf were obtained by repeated aneroid altimeter ties with McMurdo station. Pressure corrections were determined from daily weather maps and barograph data. Because of the imprecise nature of the pressure maps and the great distance from the barograph station, it is difficult to estimate accurately the uncertainty in the absolute elevations. For the areas most distant from McMurdo station errors may exceed ± 50 m.; however, greater accuracy was realized for closer stations. Relative elevation differences across the glaciers were obtained with greater precision from theodolite and altimeter measurements referred to the glacier margins. These relative profiles were adjusted to the less precise sea-level datum values at ice-shelf stations. Table I gives estimates of the error in elevation for valley glaciers.

Free-air anomalies

Free-air anomalies were computed for all stations. The accuracy of these was estimated from the elevation error and the constant 0.3086 mgal m^{-1} . Values of observed gravity, station positions and elevations, and free-air anomalies are tabulated in the Appendix.

COMPUTATION OF VALLEY CROSS-SECTIONS

The method

Valley cross-sections for the glaciers were computed from free-air anomalies corrected for the effect of terrain above the glacier surface (Appendix). Terrain corrections were computed by the line integral method (Hubbert, 1948) from cross-sectional sketches of valley sides made in the field. The estimated uncertainty of about 20 per cent in these corrections results from

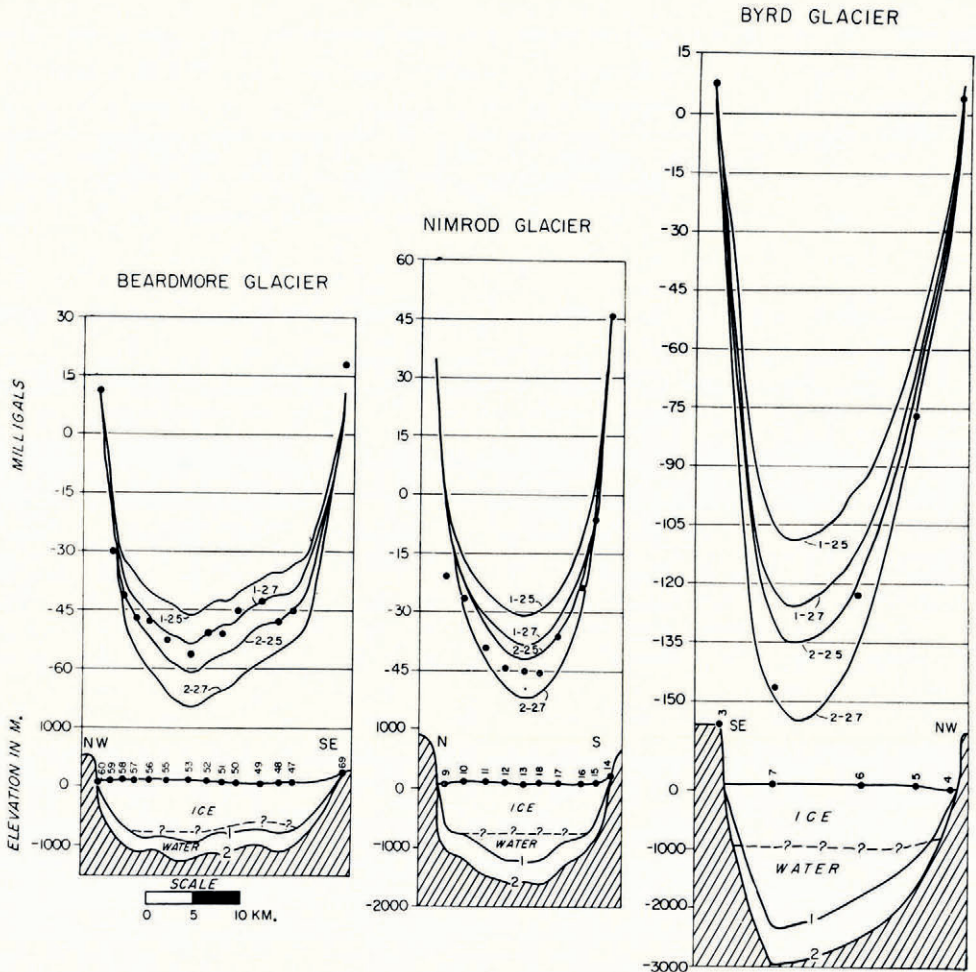


Fig. 3. Valley cross-sections and corresponding gravity profiles for floating glaciers

imprecise topographic and rock-density information. The free-air anomaly profile was assumed to be a function of subglacial rock-surface relief, which is a justifiable first approximation, because the density difference between ice (or water) and rock is much larger than contrasts between deeper rock units. Since it is reasonable to expect the average density to lie between 2.5 and 2.7 g. cm.⁻³, probable limits for subglacial rock elevation were established by computing theoretical gravity profiles for several two-dimensional valley models assigned these densities. Computations were made using the line integral approximation described by Talwani and others (1959).

Valley cross-sections

Figures 3 and 4 show two cross-sections for each valley and the corresponding gravity profiles compared with observed data. To show the possible effects due to the presence of low-density rock, calculations for Liv Glacier included an additional rock-elevation profile and an additional density value of 2.0 g. cm.^{-3} . The computed gravity profiles were tied to the observed anomalies at the glacier margins. Since these profiles include most of the free-air anomalies, the cross-sections indicate the range within which true rock elevations lie. It is

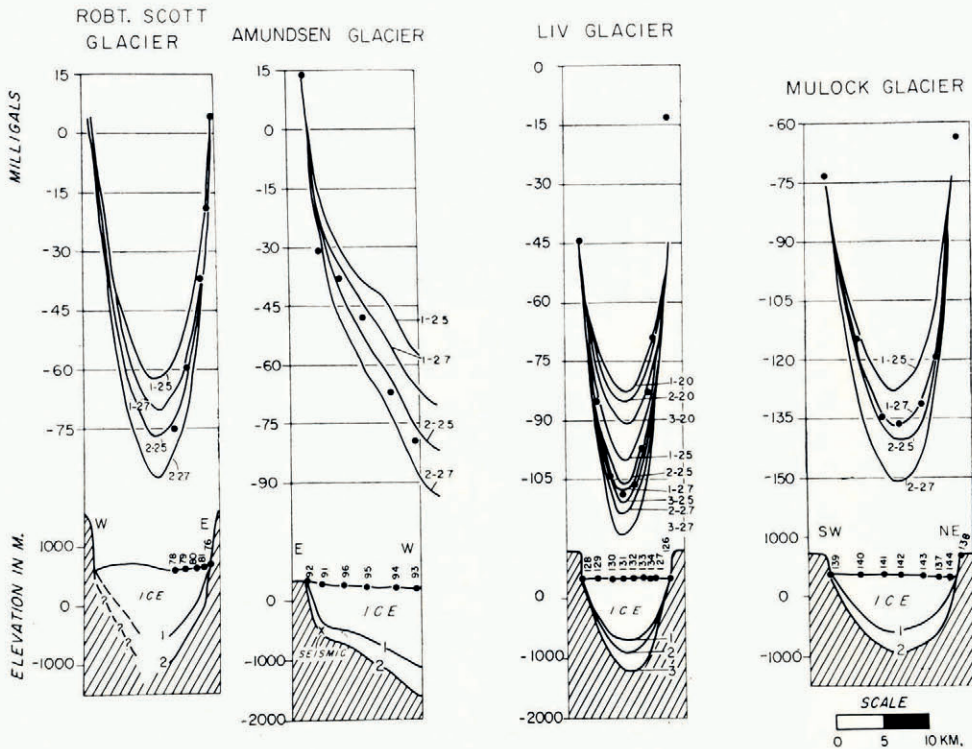


Fig. 4. Valley cross-sections and corresponding gravity profiles for grounded glaciers

not justifiable to assume a narrower density range, and therefore it is not possible to estimate the elevation of the rock surface more precisely. A few observed values are not enclosed by the theoretical profiles; they probably result from the regional gravity anomaly along the western margin of the Ross Ice Shelf (Robinson, unpublished). Because the gravity meter measures change in a potential field gradient caused by nearby relief as well as that immediately beneath it, the analysis gives smoothed valley cross-sections with minimal indication of local subglacial features. The reliability of ice-thickness values (or valley depths where the glaciers are afloat; Fig. 3) determined from gravity data is assessed using data obtained by seismic-reflection measurements. One seismic measurement near the margin of Amundsen Glacier indicates a true rock elevation between the two profiles assumed for gravity calculations. The reliability of this method of computing valley cross-sections can be further considered by examining data from Skelton Glacier (Wilson and Crary, 1961). Figure 5 shows a valley cross-section for the line of observation points given in Figure 2. Seismic-reflection measurements were made at seven sites, and corresponding free-air anomalies were obtained at these

and two additional points. Four theoretical gravity profiles were computed for this cross-section for assumed average rock densities of 2.3, 2.4, 2.5 and 2.7 g. cm.⁻³. These relative profiles were adjusted to observed free-air anomalies at the two most widely separated seismic sites: stations 61.2 and 61.6 (see circled points in Figure 5). The comparison of these profiles with observed anomalies at intermediate sites indicates that average rock density for the lower central part of the valley is between 2.3 and 2.4 g. cm.⁻³. Rock elevation was not precisely known near the glacier margins (sites 61.7 and 61.8), and an estimate of the average density along the steeper slopes near the sides of the valley cannot be obtained. It is reasonable to

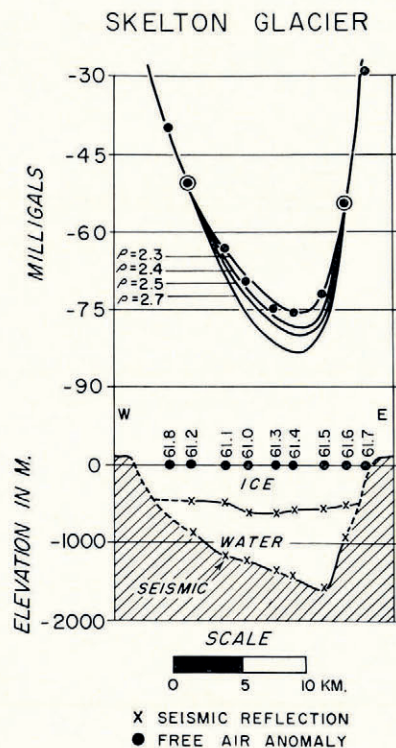


Fig. 5. Valley cross-section and corresponding gravity profiles for Skelton Glacier

expect a higher average density since a thinner low-density moraine would be expected on the steep slopes than in the center of the valley. Hence, there is justification in assuming a higher average density when calculating valley cross-sections from gravity profiles adjusted to observed values at the margins.

MEASURED ICE DISCHARGE

Areas of vertical cross-sections of ice, computed from the valley models, are given in Table I. The ice thickness of floating glaciers was calculated from surface elevation. Possible elevation error for floating ice and the two limiting profiles of rock elevation for the grounded ice are the basis for the estimates of uncertainty. To obtain the estimates of rates of ice discharge (Table I), values of average surface velocity, computed from triangulation measurements of stakes on glacier surfaces by Swithinbank (1963), were used with areas of cross-sections. The area of the western half of the cross-section of Amundsen Glacier was estimated

by extrapolation; the probable error is about 50 per cent. Table I also includes data of Wilson and Crary (1961) for Skelton Glacier.

TABLE I. ACCURACY OF ELEVATION MEASUREMENTS USED IN THE REDUCTION OF GRAVITY DATA, AND ESTIMATED ERRORS IN THE MEASUREMENTS OF ICE DISCHARGE

Glacier	Error in elevation		Ice discharge		
	Relative to sea-level	Relative to glacier margin	Area of cross-section km. ²	Mean surface velocity* km. yr. ⁻¹	Ice output km. ³ yr. ⁻¹
	m.	m.			
Robert Scott Glacier	±30	±1	11.3 ± 2.2	0.18 ± 0.01	2.0 ± 0.4
Amundsen Glacier	±30	±6	22.0 ± 11.0	0.15 ± 0.01	3.3 ± 1.7
Liv Glacier	±30	±1	6.9 ± 1.2	0.07 ± 0.01	0.5 ± 0.1
Beardmore Glacier	±10	±1	17.5 ± 5.3	0.33 ± —	5.8 ± 1.7
Nimrod Glacier	±10	±5	14.8 ± 4.4	0.15 ± —	2.2 ± 0.7
Byrd Glacier	±50	±50	22.0 ± 14.3	0.74 ± 0.01	16.3 ± 10.6
Mulock Glacier	±15	±15	9.7 ± 1.6	0.29 ± —	2.8 ± 0.5
Skelton Glacier †	?	?	9.2 ± ?	0.09 ± ?	0.8 ± ?
Measured discharge (total)					33.7 ± 10.9

* After Swithinbank (1963).

† Wilson and Crary (1961).

In the sections where movement was measured on Beardmore, Nimrod, Byrd and Skelton Glaciers, the ice was afloat. Although surface velocity is probably representative of average velocity for floating ice, this is not true for grounded ice. Nothing is known about longitudinal slope or bed roughness for the glaciers, and so the average velocity for grounded glaciers cannot be estimated; therefore, the estimates of discharge represent upper limits. The total ice discharge through the eight glaciers is 33.7 ± 10.9 km.³ yr.⁻¹, or approximately $(30 \pm 7) \times 10^{15}$ g. yr.⁻¹, using a mean density of 0.9 g. cm.⁻³ for the ice and firn. In the determination the individual errors for ice discharge were treated as standard errors. Unless otherwise specified, all errors are expressed as standard errors.

THE REGIME AND THE MASS BUDGET

The net mass budget for the western part of the Ross Ice Shelf drainage system is the difference between the rate of net mass accumulation at the surface and the rate of mass output at the drainage periphery. The drainage periphery is the boundary of grounded ice lying between Cape Chocolate (lat. 77° 58' S., long. 164° 37' E.) and the north-western extremity of Supporting Party Mountain (approximately lat. 85° 27' S., long. 147° 50' W.).

NET MASS ACCUMULATION AT THE SURFACE

Taking into account the area of net ablation at the surface in regions where surface slope favors snow deflation and a composite error due to uncertainties in the determination of mean accumulation (21 per cent) and area (15 per cent) for the whole Ross Ice Shelf drainage system (Giovinetto, 1964[a]), the rate of total accumulation for the drainage system is estimated to be $(96 \pm 25) \times 10^{15}$ g. yr.⁻¹. The mean accumulation is 5.5 ± 1.2 g. cm.⁻² yr.⁻¹, and the area is $(1.75 \pm 0.26) \times 10^6$ km.² (Giovinetto, 1964[b]). The mean accumulation data selected for particular locations are those obtained using two different methods (Crary, 1963; Giovinetto, 1963). These values were selected in preference to greater mean values for particular locations which were reported in earlier studies (Lister, 1960).

MASS OUTPUT AT THE DRAINAGE PERIPHERY

Glacier width

For purposes of extrapolating values of ice discharge the combined widths have been estimated at the drainage periphery of glaciers classified into four categories. The estimates were made from the chart of Antarctica (1 : 3,000,000; 1962) compiled by the American

Geographical Society, supplemented by recent aerophotographic material (Seelig, 1964; Swithinbank, 1964). Examination of photographs indicates that estimates based upon the chart alone would be about 15 per cent too large. The four glacier categories are described below and the combined widths of glaciers in each are given. (i) Outlet glaciers draining large inland basins are Robert Scott, Amundsen, Shackleton, Beardmore, Nimrod, Byrd and Mulock Glaciers (Swithinbank, 1964). They have a combined width of 125 km. at the drainage periphery. (ii) Outlet glaciers draining small inland basins are Isaiah Bowman, Axel Heiberg, Liv, Lennox-King, Darwin and Skelton Glaciers with a combined width of 80 km. (Fig. 2). (iii) Thirteen glaciers are classified as "cirque" glaciers in this discussion. These glaciers drain regions limited by the drainage periphery and the main ridge of the Trans-Antarctic Mountains which are not drained by tributaries to the outlet glaciers. Their combined width is 140 km. (iv) "Piedmont" glaciers flowing eastward from the main ridge of the Trans-Antarctic Mountains principally between lat. $80^{\circ} 45'$ and $82^{\circ} 10' S$. have a combined width of 250 km.

The error in the estimate of total width of the glaciers is approximately 10 per cent, although it is greater for individual glaciers where mapping is inadequate. Nine relatively small cirque glaciers with a total width of 40 km. are shown in the American Geographical Society's chart. They were excluded from this study because their topography inland is totally unknown; according to the chart they intersect the drainage periphery at approximately lat. $88^{\circ} 50' S$. (one), $83^{\circ} S$. (two), $83^{\circ} 25' S$. (one), and between lat. $84^{\circ} 30'$ and $84^{\circ} 50' S$. (five).

Mass output in outlet glaciers (large basins)

The glaciers listed in Table I (with exception of Liv and Skelton Glaciers) are representative of outlet glaciers draining large basins. The extrapolated value of ice discharge based on the total width of all outlet glaciers is $35.4 \pm 10.9 \text{ km.}^3 \text{ yr.}^{-1}$ or $(32 \pm 10) \times 10^{15} \text{ g. yr.}^{-1}$. The rate of ice discharge for Shackleton Glacier is estimated to be $3.0 \pm 0.6 \text{ km.}^3 \text{ yr.}^{-1}$, assuming a mean ice discharge for the outlet glaciers of $0.19 \pm 0.4 \text{ km.}^3 \text{ km.}^{-1} \text{ yr.}^{-1}$. The mean ice discharge per kilometer and the error for Shackleton Glacier are estimated using the smaller of the two magnitudes of ice discharge evident in Table I. The mean for Robert Scott, Amundsen, Beardmore, Nimrod and Mulock Glaciers is approximately $0.19 \text{ km.}^3 \text{ km.}^{-1} \text{ yr.}^{-1}$. The mean for Byrd Glacier is approximately $0.68 \text{ km.}^3 \text{ km.}^{-1} \text{ yr.}^{-1}$.

Mass output in outlet glaciers (small basins)

Using the data from Liv and Skelton Glaciers, the mean ice discharge for outlet glaciers draining relatively small basins is estimated to be approximately $0.05 \pm 0.02 \text{ km.}^3 \text{ km.}^{-1} \text{ yr.}^{-1}$ (the error of 38 per cent is estimated simply by doubling the error computed for ice discharge in Liv Glacier). Hence, their contribution to the ice shelf is $4.0 \pm 1.5 \text{ km.}^3 \text{ yr.}^{-1}$ or $(4 \pm 1) \times 10^{15} \text{ g. yr.}^{-1}$.

Mass output in "cirque" and "piedmont" glaciers

No measurements of ice discharge have been made on cirque and piedmont glaciers, but the rate of mass output can be estimated from the snowshed area and the corresponding rate of accumulation. The drainage periphery is approximately 1,100 km. long, and includes 205 km. of outlet glaciers, 250 km. of piedmont glaciers, and 140 km. of cirque glaciers. The remaining 500 km. correspond to the perimeter of narrow capes and peninsulas where mass movement is parallel to the drainage periphery, tributary glaciers feeding into outlet and cirque glaciers. These tributary glaciers are of three main types, i.e. valley, cirque and hanging glaciers.

The piedmont glaciers flow eastward on the flanks of the Trans-Antarctic Mountains, principally between lat. $80^{\circ} 45'$ and $82^{\circ} 10' S$. They drain an area which extends directly inland from the drainage periphery to the main ridge of the Trans-Antarctic Mountains; these

lie, in general, between 50 and 100 km. from each other. Hence the combined snowshed area of $19,000 \pm 6,000 \text{ km.}^2$ is obtained from the periphery width of 250 km. and the inland extent of $75 \pm 25 \text{ km.}$ The estimated mean net accumulation of $25 \pm 5 \text{ g. cm.}^{-2} \text{ yr.}^{-1}$ (Giovinetto, 1963, 1964[a]) and the assumption that the piedmont glaciers are in a situation of steady-state determine the total mass output to be $(5 \pm 2) \times 10^{15} \text{ g. cm.}^{-2} \text{ yr.}^{-1}$.

The remaining 850 km. of the drainage periphery and the main ridge of the Trans-Antarctic Mountains ($75 \pm 25 \text{ km.}$ apart) limit an area of $64,000 \pm 21,000 \text{ km.}^2$. Here tributary glaciers drain into outlet and cirque glaciers. Such a discharge into outlet glaciers has already been accounted for; it remains to estimate the ice discharge by tributary glaciers into cirque glaciers. It is assumed that from the combined snowshed area of $64,000 \pm 28,000 \text{ km.}^2$ the area of regions drained through tributaries by cirque and outlet glaciers is proportional to the width of these glaciers at the drainage periphery (140 and 205 km., respectively). Hence the total area drained by cirque glaciers is $26,000 \pm 9,000 \text{ km.}^2$. Using the estimated mean net accumulation of $25 \pm 5 \text{ g. cm.}^{-2} \text{ yr.}^{-1}$ and assuming a situation of steady-state, the rate of mass output is $(7 \pm 2) \times 10^{15} \text{ g. yr.}^{-1}$.

Total mass output

The loss of mass by surface ablation in outlet and cirque glaciers is negligible relative to the amount of total ice discharge, and has been accounted for in estimating net accumulation at the surface. The mass loss by oceanic melting from the four glaciers where the drainage periphery lies in floating sections is also negligible because: (i) Beardmore Glacier is grounded a few kilometers up-stream from the section where ice movement was measured. (ii) The remaining three glaciers, with a total width of only 55 km. are probably grounded inland from the main ridge of the Trans-Antarctic Mountains. If the rate of bottom melting in these glaciers is one-half the rate estimated by Crary (1964) for "Little America V" (Fig. 1), i.e. $30 \text{ g. cm.}^{-2} \text{ yr.}^{-1}$, mass loss by oceanic melting is about $10^{15} \text{ g. yr.}^{-1}$. This value was neglected as it would not change the estimates of ice discharge by outlet and cirque glaciers at the drainage periphery (grounded ice).

From the factors given, the total mass flux at the 1,100 km. long periphery is estimated to be $(48 \pm 15) \times 10^{15} \text{ g. yr.}^{-1}$.

Mass flux

Despite the relatively low rate of mass output, exceptionally high rates of ice movement in some of the outlet glaciers and correspondingly great mass flux occur (Swithinbank, 1964), caused by the damming effect of the Trans-Antarctic Mountains. Mean mass flux at the drainage periphery is estimated at $(0.04 \pm 0.01) \times 10^{15} \text{ g. km.}^{-1} \text{ yr.}^{-1}$; this rate is relatively low compared with the mean mass flux for the periphery of the grounded ice sheet in Antarctica ($(0.9 \pm 0.5) \times 10^{15} \text{ g. km.}^{-1} \text{ yr.}^{-1}$; Giovinetto, 1964[b]). From the discussion on estimating values of ice discharge for different types of glaciers the following mean values of mass flux are deduced: mass flux in outlet glaciers with large drainage basins is approximately $0.25 \times 10^{15} \text{ g. km.}^{-1} \text{ yr.}^{-1}$; in outlet glaciers with small basins and cirque glaciers it is $0.05 \times 10^{15} \text{ g. km.}^{-1} \text{ yr.}^{-1}$; and in piedmont glaciers it is $0.02 \times 10^{15} \text{ g. km.}^{-1} \text{ yr.}^{-1}$. The values of mass flux at the grounded (or close to grounded) periphery sections of single glaciers listed in Table I range from less than 0.02×10^{15} to $0.68 \times 10^{15} \text{ g. km.}^{-1} \text{ yr.}^{-1}$. Factors greater than 30 between mean values of mass flux for single glaciers and greater than 10 between mean values for particular glacier types demonstrate the physiographic complexity of the drainage periphery.

NET BUDGET

The difference between the estimates of mass input ($(96 \pm 25) \times 10^{15} \text{ g. yr.}^{-1}$) and mass output ($(48 \pm 15) \times 10^{15} \text{ g. yr.}^{-1}$) suggests a positive net budget ($(48 \pm 29) \times 10^{15} \text{ g. yr.}^{-1}$).

It would be unrealistic to make a rigorous significance test on the net budget estimate because the "mean" values of mass input and output are estimates based on sets of heterogeneous data, and the standard errors are estimates themselves. Nevertheless, the net budget estimate is 1.7 times the standard error, including a large probability that the net budget is different from zero.

CONCLUDING REMARKS

The preceding discussion, stressing the errors in all estimates and the magnitude of the standard error, shows that a net budget of 50 per cent is not significant. This has been stated before regarding Antarctic drainage systems (Giovinetto, 1964[a]).

The present estimate of the net budget might be questioned, because the data cover periods of 2 yr. (mass output) and 5 yr. (mass input). The temporal variability of the rate of mass output is unknown, but it is reasonable to assume that it would be less variable than the rate of mass input which can be estimated. The variability of the rate of precipitation decreases as the area for which the variability is estimated increases (e.g. Schwerdtfeger, 1951). A correlation study of accumulation data for periods longer than 100 yr. at three stations shown in Figure 1, i.e. South Pole (Giovinetto, 1960), Wilkes S-2 (Cameron and others, 1959; Fig. 1) and "Little America V" (Gow, 1963) indicates that the variability of 10 yr. means of net accumulation at the surface for comparable areas is approximately 2 per cent (personal communication from W. Schwerdtfeger) or 3 per cent for 5 yr. means. Evidently the difference between the rates of mass input and mass output cannot be caused completely by their variability.

There is no evidence of a significant secular change in the rates of mass input and output which would justify re-estimating the net budget. Approximately one-half the amount of the total mass input corresponds to a 200 km. wide zone adjacent to the drainage periphery (Giovinetto, 1963). A significant change in the rate of mass input should be detectable as a change in the rate of mass output after a few decades, certainly less than 100 yr. (e.g. Weertman, 1958). However, in a study of the significant increase in the rate of accumulation at the South Pole between 1760 and 1957 (Giovinetto and Schwerdtfeger, 1966), it is shown that there were no significant changes in the rate of accumulation for comparable periods at "Little America V" and Wilkes S-2 (Fig. 1). Hence there is evidence to support a secular increase in the rate of accumulation only in the southern part of the system where accumulation is small.

ACKNOWLEDGEMENTS

The field work and data analysis were supported by grants from the National Science Foundation to the University of Michigan and the University of Wisconsin. Logistics support was provided by the U.S. Navy. Individuals whose help in field work or in data reduction made this work possible are: D. G. Darby, E. Dorrer, D. Lavin, O. Liestøl, H. W. Linder, J. J. Olson, A. S. Rundle, T. E. Taylor, E. Thiel (deceased) and J. Tuck. It is a pleasure to acknowledge the critical review of the manuscript by C. R. Bentley, K. W. Butzer and W. Schwerdtfeger.

MS. received 3 March 1965

REFERENCES

- Cameron, R. L., and others. 1960. Wilkes station glaciological data, by R. L. Cameron, O. H. Løken and J. R. T. Molholm. *Ohio State University Research Foundation. Report 825-1-III.*
- Crary, A. P. 1963. Results of United States traverses in East Antarctica, 1958-1961. *IGY Glaciological Report* (New York), No. 7.
- Crary, A. P. 1964. Melting at the ice-water interface, "Little America" station. *Journal of Glaciology*, Vol. 5, No. 37, p. 129-30. [Letter.]

Giovinetto, M. B. 1960. Glaciology report for 1958, South Pole station. *Ohio State University Research Foundation. Report 825-2-IV.*

Giovinetto, M. B. 1963. Glaciological studies on the McMurdo-South Pole traverse, 1960-61. *Ohio State University. Institute of Polar Studies. Report No. 7.*

Giovinetto, M. B. 1964[a]. The drainage systems of Antarctica: accumulation. (*In Mellor, M., ed. Antarctic snow and ice studies.* Washington, D.C., American Geophysical Union, p. 127-55. (Antarctic Research Series, Vol. 2.))

Giovinetto, M. B. 1964[b]. An estimate of mass flux, Antarctica. *Geological Society of America. Special Papers*, No. 76, p. 309. [Abstract.]

Giovinetto, M. B., and Schwerdtfeger, W. 1966. Analysis of a 200-year snow accumulation series from the South Pole. *Archiv für Meteorologie, Geophysik und Bioklimatologie*, Ser. A, Bd. 15, Ht. 2. [In press, January 1966.]

Gow, A. J. 1963. The inner structure of the Ross Ice Shelf at Little America V, Antarctica, as revealed by deep core drilling. *Union Géodésique et Géophysique Internationale. Association Internationale d'Hydrologie Scientifique. Assemblée générale de Berkeley, 19-8-31-8 1963. Commission des Neiges et des Glaces*, p. 272-84.

Hubbert, M. K. 1948. A line integral method of computing the gravimetric effects of two-dimensional masses. *Geophysics*, Vol. 13, No. 2, p. 215-25.

Lister, H. 1960. Glaciology. 1. Solid precipitation and drift snow. *Trans-Antarctic Expedition, 1955-1958. Scientific Reports*, No. 5.

Robinson, E. S. Unpublished. Geological structure of the Transantarctic Mountains and adjacent ice covered areas, Antarctica. [Ph.D. thesis, University of Wisconsin, 1964.]

Schwerdtfeger, W. 1951. Gedanken über ein Ausgleichsprinzip des atmosphärischen Gesamt-Niederschlags. *Meteorologische Rundschau*, Bd. 4, Ht. 5/6, p. 96-97.

Seelig, W. R. 1964. Topographic mapping of Antarctica. *Antarctic Report* (Washington, D.C.), June 1964, p. 2-18.

Swithinbank, C. W. M. 1963. Ice movement of valley glaciers flowing into the Ross Ice Shelf, Antarctica. *Science*, Vol. 141, No. 3580, p. 523-24.

Swithinbank, C. W. M. 1964. The valley glaciers that feed the Ross Ice Shelf. *Polar Record*, Vol. 12, No. 76, p. 80-82.

Talwani, M., and others. 1959. Rapid gravity computations for two-dimensional bodies with application to the Mendocino submarine fracture zone, by M. Talwani, J. L. Worzel and M. Landisman. *Journal of Geophysical Research*, Vol. 64, No. 1, p. 49-60.

Weertman, J. 1958. Traveling waves on glaciers. *Union Géodésique et Géophysique Internationale. Association Internationale d'Hydrologie Scientifique. Symposium de Chamorix, 16-24 sept. 1958*, p. 162-68.

Wilson, C. R., and Cray, A. P. 1961. Ice movement studies on the Skelton Glacier. *Journal of Glaciology*, Vol. 3, No. 29, p. 873-78.

APPENDIX

GRAVITY VALUES: 1961-62 ROSS ICE SHELF GLACIOLOGY TRAVERSE

Glacier	Station	Position		Observed gravity gal	Elevation m.	Free-air anomaly mgal	Terrain correction mgal	Terrain-corrected free-air anomaly mgal
		lat. S.	long.					
	1R*	77° 50.9'	166° 40'E.	982.9885	29	+6.3		
	2	77° 52.2'	166° 28'	982.9682	1	-23.4		
Byrd Glacier (adjusted to station 3) station 3 adjusted 1,000 m. down	3R	80° 11.5'	159° 15'	982.7783	1,136	+58.4	-50	+8
	4	80° 24.0'	159° 54'	983.0454	54	-14.7	+20	+5
	5	80° 21.9'	159° 47'	982.9552	102	-89.0	+12	-77
	6	80° 19.1'	159° 40'	982.9135	101	-129.7	+6	-123
	7	80° 15.1'	159° 24'	982.8866	95	-156.5	+11	-146
	8	82° 19.5'	164° 06'	983.0491	101	-44.3		
Nimrod Glacier (adjusted to station 14)	9	82° 15.0'	163° 44'	983.0550	99	-41.2	+20	-21
	10	82° 15.9'	163° 47'	983.0500	126	-38.3	+12	-26
	11	82° 16.9'	163° 51'	983.0416	123	-48.0	+9	-39
	12	82° 17.9'	163° 57'	983.0425	107	-52.5	+9	-44
	13	82° 18.5'	163° 59'	983.0503	81	-52.9	+9	-44
	14R	82° 23.3'	164° 18'	983.0772	229	+17.8	+28	+46
	15	82° 22.5'	164° 02'	983.0730	100	-25.9	+20	-6
	16	82° 21.6'	164° 05'	983.0657	93	-35.0	+12	-23
	17	82° 20.5'	164° 05'	983.0524	104	-44.5	+9	-36
	18	82° 20.0'	163° 59'	983.0423	101	-55.3	+9	-46
	19	82° 18.9'	164° 18'	983.0615	101	-35.7		
	20	82° 18.3'	164° 30'	983.0686	91	-31.4		
21	82° 17.6'	164° 42'	983.0775	87	-23.5			

* The symbol "R" designates gravity stations on outcropping rock.

Glacier	Station	Position		Observed gravity gal	Elevation m.	Free-air anomaly mgal	Terrain correction mgal	Terrain- corrected free-air anomaly mgal
		lat. S.	long.					
	22	82° 16.7'	164° 55'	983.0816	80	-21.2		
	23	82° 15.3'	165° 03'	983.0855	80	-16.7		
	24	82° 13.9'	165° 11'	983.0883	80	-38.1		
	25	82° 12.5'	165° 18'	983.0856	78	-16.1		
	26	82° 11.0'	165° 25'	983.0834	78	-17.7		
	27	82° 09.6'	165° 30'	983.0841	70	-18.9		
	28	82° 07.8'	165° 30'	983.0842	72	-17.5		
	29	82° 07.2'	165° 35'	983.0836	73	-17.6		
	30	82° 07.4'	165° 45'	983.0882	51	-19.9		
	31	82° 07.7'	165° 55'	983.0889	46	-20.8		
	32	82° 08.2'	166° 05'	983.0893	50	-19.4		
	33	82° 08.4'	166° 10'	983.0890	53	-18.8		
	34	82° 22.2'	167° 17'	983.1106	44	-5.5		
	35	82° 34.3'	168° 41'	983.1099	53	-8.2		
	36	82° 38.8'	166° 04'	983.1129	48	-8.6		
	37	82° 44.8'	166° 36'	983.1149	44	-10.1		
	38	82° 48.6'	169° 58'	983.1113	44	-15.0		
	39	82° 53.3'	170° 35'	983.1108	46	-16.7		
	40	82° 58.0'	171° 13'	983.1125	53	-14.5		
	41	83° 03.3'	171° 58'	983.1192	56	-8.8		
	42	83° 07.3'	172° 32'	983.1212	55	-8.6		
	43	83° 13.2'	173° 45'	983.1216	62	-8.2		
	44	83° 17.7'	174° 24'	983.1259	56	-7.3		
	45	83° 20.9'	174° 54'	983.1275	57	-6.5		
	46	83° 35.8'	172° 08'	983.0769	100	-48.8		
Beardmore Glacier (ad- justed to stations 60 and 69)	47	83° 40.1'	172° 29'	983.0859	89	-44.7	0	-45
	48	83° 39.3'	172° 27'	983.0841	85	-47.5	0	-48
	49	83° 38.3'	172° 26'	983.0958	61	-42.9	0	-43
	50	83° 37.1'	172° 21'	983.0867	81	-45.4	0	-45
	51	83° 36.7'	172° 13'	983.0790	93	-49.6	0	-50
	52	83° 36.1'	172° 04'	983.0752	101	-50.3	0	-50
	53	83° 35.5'	171° 56'	983.0659	111	-56.4	0	-56
	54	83° 35.2'	171° 59'	983.0679	107	-55.6		
	55	83° 34.2'	171° 54'	983.0700	104	-54.1	0	-53
	56	83° 33.2'	171° 48'	983.0755	101	-49.1	0	-48
	57	83° 33.1'	171° 38'	983.0773	100	-47.7	0	-47
	58	83° 32.8'	171° 30'	983.0839	93	-43.0	0	-41
	59	83° 32.5'	171° 53'	983.0874	108	-34.9	0	-30
	60	83° 31.1'	171° 30'	983.1305	86	+1.9	0	+11
	61	83° 34.0'	172° 23'	983.0881	90	-40.2		
	62	83° 32.6'	172° 42'	983.0919	87	-36.9		
	63	83° 31.1'	173° 02'	983.1023	77	-29.0		
	64	83° 29.9'	173° 22'	983.1104	71	-22.4		
	65	83° 28.5'	173° 42'	983.1158	70	-16.8		
	66	83° 27.0'	174° 01'	983.1223	56	-14.1		
	67	83° 25.1'	174° 17'	983.1251	60	-9.4		
	68	83° 23.3'	174° 33'	983.1262	65	-6.1		
Beardmore Glacier	69R	83° 42.9'	172° 42'	983.1001	262	+21.6	0	+22
	70	83° 28.5'	176° 22'	983.1339	51	-4.6		
	71	83° 24.8'	175° 37'	983.1305	58	-4.6		
	72	84° 58.1'	158° 52' W.	983.1237	115	-22.1		
	73	85° 08.2'	155° 26'	983.1178	115	-30.6		
	74	85° 23.3'	151° 41'	983.1090	135	-37.0		
	75	85° 30.5'	151° 13'	983.1028	290	+2.8		
Robert Scott Glacier (ad- justed to station 76)	76R	85° 43.7'	152° 04'	982.9906	640	-4.3	+9	+5
	77	85° 43.7'	152° 04'	982.9890	643	-5.0		
	78	85° 43.8'	152° 31'	982.9042	685	-76.9	+2	-75
	79	85° 42.8'	152° 23'	982.9351	633	-61.9	+3	-59
	80	85° 42.8'	152° 11'	982.9569	631	-40.7	+5	-36
	81	85° 43.1'	152° 06'	982.9708	639	-24.3	+7	-19

Glacier	Station	Position		Observed gravity gal	Elevation m.	Free-air anomaly mgal	Terrain correction mgal	Terrain-corrected free-air anomaly mgal
		lat. S.	long.					
	82	85° 28.2'	151° 20'	983.0821	257	-27.5		
	83	85° 25.9'	151° 30'	983.0981	229	-19.6		
	84	85° 21.3'	151° 49'	983.1012	122	-48.5		
	85	85° 19.6'	152° 11'	983.0788	120	-71.0		
	86	85° 17.5'	152° 35'	983.0719	118	-78.0		
	87	85° 15.4'	152° 57'	983.0756	115	-74.7		
	88	85° 14.3'	153° 26'	983.0805	113	-71.1		
	89	85° 13.1'	153° 54'	983.0867	111	-64.2		
	90	85° 20.0'	156° 11'	983.1433	84	-17.7		
Amundsen Glacier (adjusted to station 92). Seismic reflection recorded rock elevation of -450 m. at station 91	91	85° 25.2'	156° 54'	983.0713	279	-30.7	0	-31
	92R	85° 24.6'	156° 45'	983.1062	310	+13.9	0	+14
	93	85° 25.3'	158° 03'	983.0525	180	-80.2	0	-80
	94	85° 25.2'	157° 46'	983.0605	196	-67.1	0	-67
	95	85° 25.0'	157° 27'	983.0700	227	-48.0	0	-48
	96	85° 24.9'	157° 10'	983.0727	251	-37.9	0	-38
	97	85° 23.4'	156° 39'	983.1208	233	+5.0		
	98	85° 21.6'	156° 49'	983.1354	149	-5.9		
	99	85° 19.2'	157° 02'	983.1345	115	-16.8		
	100	85° 17.0'	157° 15'	983.1249	105	-28.9		
	101	85° 14.9'	157° 26'	983.1273	108	-25.1		
	102	85° 12.5'	157° 39'	983.1290	111	-21.8		
	103	85° 10.1'	157° 52'	983.1314	115	-17.5		
	104	85° 07.8'	158° 03'	983.1337	114	-15.0		
	105	85° 05.5'	158° 15'	983.1314	112	-17.3		
	106	85° 03.2'	158° 26'	983.1272	114	-20.3		
	107	85° 00.9'	158° 36'	983.1237	113	-23.5		
	108	84° 59.4'	159° 16'	983.1194	122	-24.7		
	109	85° 00.5'	159° 38'	983.1158	131	-25.8		
	110	85° 01.7'	160° 03'	983.0995	145	-38.1		
	111	85° 02.9'	160° 27'	983.0935	129	-49.3		
	112	85° 03.9'	160° 52'	983.0861	127	-57.7		
	113	85° 05.0'	161° 17'	983.0976	138	-42.9		
	114	85° 06.1'	161° 42'	983.1011	158	-33.5		
	115	85° 07.2'	162° 09'	983.0886	200	-33.4		
	116	85° 08.2'	162° 32'	983.0853	206	-35.0		
	117R	85° 10.1'	163° 17'	983.0736	361	+0.6		
	118	85° 09.7'	163° 30'	982.9879	514	-37.8		
	119	85° 08.5'	163° 55'	983.0226	487	-11.2		
	120	85° 07.2'	164° 19'	983.0303	441	-17.3		
	121	85° 04.9'	164° 28'	983.0424	398	-17.9		
	122	85° 02.8'	164° 44'	983.0541	350	-20.5		
	123	85° 00.8'	164° 56'	983.0698	287	-23.7		
	124	84° 58.7'	165° 11'	983.0782	249	-26.5		
	125	84° 57.0'	165° 21'	983.0806	228	-30.0		
Liv Glacier (adjusted to stations 126 and 128)	126R	84° 55.4'	167° 29'	983.0408	351	-31.5	+18	-13
	127	84° 55.9'	167° 39'	982.9921	361	-77.3	+8	-69
	128R	84° 54.7'	168° 26'	983.0186	325	-61.6	+18	-44
	129	84° 54.7'	168° 17'	982.9836	333	-94.1	+9	-85
	130	84° 54.8'	168° 07'	982.9712	318	-111.2	+7	-104
	131	84° 55.2'	168° 00'	982.9639	329	-115.2	+6	-109
	132	84° 55.4'	167° 54'	982.9653	332	-112.9	+6	-107
	133	84° 55.8'	167° 47'	982.9653	364	-103.2	+6	-97
	134	84° 56.1'	167° 42'	982.9761	372	-89.9	+7	-83
	135R	77° 50.9'	166° 40' E.	982.9886	26	+5.5		
	136R	77° 51.0'	166° 40'	982.9919	11	+4.1		
	137	79° 04.8'	160° 10'	982.7912	349	-136.0		
Mulock Glacier (adjusted to station 139). Station 138 was adjusted 320 m. down	138	79° 06.4'	160° 07'	982.7787	682	-46.6	-18	-65
	139	79° 00.5'	160° 32'	982.8302	362	-90.6	+18	-73
	140	79° 01.9'	160° 26'	982.7992	371	-119.5	+5	-115
	141	79° 02.9'	160° 22'	982.7803	376	-137.5	+4	-134

<i>Glacier</i>	<i>Station</i>	<i>Position</i>		<i>Observed gravity gal</i>	<i>Elevation m.</i>	<i>Free-air anomaly mgal</i>	<i>Terrain correction mgal</i>	<i>Terrain- corrected free-air anomaly mgal</i>
		<i>lat. S.</i>	<i>long.</i>					
	142	79° 03·7'	160° 18'	982·7786	375	-139·9	+3	-137
	143	79° 04·8'	160° 13'	982·7899	352	-136·4	+5	-131
	144	79° 05·5'	160° 10'	982·8066	335	-125·3	+7	-118

GRAVITY VALUES: 1958-59 "LITTLE AMERICA V"-VICTORIA LAND TRAVERSE

Skelton Glacier	61.0	79° 00·0'	162° 14'E.	982·9368	84	-69·4	0	-69
	61.1	79° 00·6'	162° 10'	982·9476	71	-63·1	0	-63
	61.2	79° 01·2'	162° 06'	982·9609	70	-50·4	0	-50
	61.3	78° 59·2'	162° 17'	982·9308	84	-75·0	0	-75
	61.4	78° 58·5'	162° 21'	982·9307	80	-75·9	0	-76
	61.5	78° 57·8'	162° 25'	982·9347	78	-72·2	0	-72
	61.6	78° 57·2'	162° 28'	982·9528	76	-54·3	0	-54
	61.7	78° 56·5'	162° 32'	982·9783	72	-29·7	0	-30
	61.8	79° 01·7'	162° 02'	982·9733	66	-39·5	0	-40